Matter-wave soliton bouncing on a reflecting surface under the effect of gravity

A. Benseghir,[1] W. A. T. Wan Abdullah,[1] B. B. Baizakov,[2] and F. Kh. Abdullaev[3]
[1]*Department of Physics, Faculty of Science, University of Malaya, 50603, Kuala Lumpur, Malaysia*
[2]*Physical-Technical Institute, Uzbek Academy of Sciences, 100084, Tashkent, Uzbekistan*
[3]*Department of Physics, Faculty of Science, International Islamic University of Malaysia, 25200, Kuantan, Malaysia*
(Received 22 June 2014; published 6 August 2014)

The dynamics of a matter-wave soliton bouncing on the reflecting surface (atomic mirror) under the effect of gravity has been studied by analytical and numerical means. The analytical description is based on the variational approach. Resonant oscillations of the soliton's center of mass and width, induced by appropriate modulation of the atomic scattering length and the slope of the linear potential, are analyzed. In numerical experiments we observe the Fermi-type acceleration of the soliton when the vertical position of the reflecting surface is periodically varied in time. Analytical predictions are compared to the results of numerical simulations of the Gross-Pitaevskii equation and qualitative agreement between them is found.

DOI: 10.1103/PhysRevA.90.023607 PACS number(s): 03.75.Lm, 05.45.Yv

I. INTRODUCTION

A particle bouncing on the reflecting surface under the effect of gravity represents one of the analytically solvable models in quantum mechanics [1,2]. Gibbs introduced the name "quantum bouncer" [3] for the object, and it was extensively studied in many articles of pedagogical orientation [4,5] and original research papers (for a recent review see [6]). The practical interest in this model has emerged from recent experiments aimed at probing the coherence properties of Bose-Einstein condensates falling under gravity and bouncing off a mirror formed by a far-detuned sheet of light [7], quantum reflection of matter waves [8], and measuring the Casimir-Polder force acting upon the atoms near solid surfaces [9].

Another important result linked to the quantum bouncer problem has been the experimental observation of quantum bound states of neutrons in the Earth's gravitational field [10–12]. In these pioneering experiments the quantum states of matter formed by a gravitational field were observed for the first time. Also, the model is of particular interest from the viewpoints of the physics and applications of quantum states of nanoparticles in the vicinity of surfaces [13]. An optical analog of the quantum bouncer, a photon bouncing ball, was experimentally demonstrated using the circularly curved optical waveguide [14]. The significance of the model for the study of the dynamics of particles in a quantum-classical interface was pointed out in [15].

In this work we extend the quantum bouncer model to the nonlinear domain by considering the dynamics of a matter-wave soliton governed by the Gross-Pitaevskii equation (GPE). The linear potential entering the GPE represents the Earth's gravitational field acting on the soliton in the vertical direction, while the horizontal atomic mirror [16] created by a laser beam or magnetic field stands for the reflecting surface. The matter-wave soliton performs a bounded motion in such a gravitational cavity. The effect of nonlinearity, originating from the atomic interactions in the Bose-Einstein condensate (BEC), shows up as an ability of the bouncing wave packet to remain localized during the evolution, behaving like a rigid ball, rather than a deformable wave packet. The possibility of tuning the atomic interactions in the condensate by external magnetic [17] and optical [18] fields opens perspectives in exploring the bouncer problem in both the quantum and classical limits.

Our main objective is to develop analytical description of the soliton's dynamics above the atomic mirror under the effect of gravity. As an illustration of the developed model we consider the resonant oscillations of the soliton's center-ofmass position under the periodically varying strength of nonlinearity and the slope of the quasi-one-dimensional (1D) trap with respect to the horizontal reflecting surface. The strength of nonlinearity can be tuned using the Feshbach resonance technique [17], or alternatively, by changing the strength of the radial confinement. In numerical simulations we demonstrate the Fermi-type acceleration of the soliton when the vertical position of the mirror is periodically varied in time. It should be noted that Fermi acceleration of matter wave packets was previously considered in [19] for the case of noninteracting BEC, in the setting where matter-wave solitons do not exist. In these works the nondispersive acceleration of the wave packet was reported to take place under certain conditions, when the modulation strength and frequency provided the dynamical localization of the matter wave.

The advantage of the present setting is that the bouncing matter wave packet preserves its integrity due to the focusing nonlinearity of the BEC, which counteracts the dispersive spreading. Another interesting approach to the acceleration of a single quantum particle, also feasible in the context of matter waves, was reported in [20]. The mechanism consists in binding the wave packet by a δ function potential well and involving in accelerated motion along with the potential. In the linear case and ideal mirror potential our model reduces to the equation which has analytic solution in terms of Airy functions. The dynamics of Airy beams currently represents one of the actively explored topics motivated by important applications in optical communications and nonlinear optics [21].

The paper is structured as follows. In Sec. II we introduce the mathematical model and illustrate the distinctive features of the nonlinear model as compared to its linear counterpart. In Sec. III a variational approach for the analytical treatment of the nonlinear model is developed and its predictions are compared to numerical simulations of the original GPE. Section IV is devoted to exploring the resonant oscillations of the wave packet above the mirror, and the Fermi-type of

acceleration of matter-wave solitons when the vertical position of the reflecting surface is periodically varied in time. In Sec. V we summarize our findings.

II. MODEL AND MAIN EQUATIONS

The Bose-Einstein condensate is a giant matter wave packet which is strongly affected by gravity. In particular, a matter wave packet released from the trap falls towards Earth like a bunch of coherent atoms. The effect of gravity is essential for the operation of atom lasers [22].

In the present model the gravitational field acting on atoms in the vertical direction and a horizontal atom mirror which reflects them back, form a cavity for the matter wave packet. Below we consider the motion of a matter-wave soliton within such a gravitational cavity. The model is based on the following 1D GPE:

$$i\hbar\frac{\partial\psi}{\partial t} = -\frac{\hbar^2}{2m}\frac{\partial^2\psi}{\partial x^2} + mgx\psi + U(x)\psi + 2\hbar\omega_\perp a_s|\psi|^2\psi, \tag{1}$$

where $\psi(x,t)$ is the wave function of the condensate trapped in a tight quasi-1D trap, x is the spatial coordinate of the wave packet above the horizontal atomic mirror, represented by the reflecting potential $U(x)$, g is the strength of the gravitational potential, $\omega_\perp$ is the trap frequency in the tightly confining radial direction, and m,a_s are the atomic mass and s-wave scattering length, respectively.

The gravitational units of space and time, defined as

$$l_g = \left(\frac{\hbar^2}{m^2 g}\right)^{1/3}, \quad t_g = \left(\frac{\hbar}{mg^2}\right)^{1/3}, \tag{2}$$

allow to rewrite Eq. (1) in the dimensionless form

$$i\psi_t + \tfrac{1}{2}\psi_{xx} + \gamma|\psi|^2\psi - \alpha x\psi + V(x)\psi = 0, \tag{3}$$

where the new variables are defined as $x \to x/l_g$, $t \to t/t_g$, $V(x) = -U(x)/(mgl_g)$, $\psi \to \sqrt{2\omega_\perp|a_s|t_g}\psi$. Here we took into regard that for a BEC with attractive atomic interactions, $a_s < 0$. The norm of the dimensionless wave function is defined as $N = \int_{-\infty}^{\infty}|\psi(x)|^2dx$, and it is proportional to the number of atoms in the condensate. In Eq. (3) the linear potential term ($\sim x$) accounts for the effect of gravity, while the atomic mirror is represented by $V(x)$. We introduced an additional parameter $\alpha = \sin(\beta)$ to account for the possibility of altering the effect of gravity by changing the angle β formed by the axis of the quasi-1D waveguide and the horizontal reflecting surface. For vertical position ($\beta = \pi/2$) of the waveguide $\alpha = 1$, at smaller angles $0 < \beta < \pi/2$, then $0 < \alpha < 1$. Such a setting is of interest in view of recent research on the behavior of the BEC in microgravity [23] and the quantum reflection of matter waves [8], where the cold atoms should approach the attractive potential at very low velocity. Similarly, the additional parameter γ can be used for nonlinearity management $\gamma(t) = a_s(t)/a_s^0$, then in the normalization for ψ in Eq. (3) the background value of a_s^0 should be assumed. The following two cases will be relevant to our further analysis:

$$\text{(a) ideal mirror} \quad V(x) = \begin{cases} 0, & \text{if } x \geqslant 0 \\ +\infty, & \text{if } x < 0 \end{cases},$$

$$\text{(b) weakly transparent reflecting surface} \quad V(x) = V_0\delta(x), \tag{4}$$

where $\delta(x)$ is the Dirac δ function which has been multiplied by the strength V_0.

A detailed study of the wave-packet dynamics described by Eq. (3) in the linear model ($\gamma = 0$) for an ideal mirror was reported in [4]. Before proceeding to the analytical description of the nonlinear model ($\gamma = 1$) it is instructive to compare these two limits by numerical simulations of the governing equation (3). Such a preliminary study will help to elucidate the effect of nonlinearity on the dynamics of a wave packet bouncing above the atomic mirror.

In Fig. 1 we illustrate the features of the linear and nonlinear models for the dynamics of the wave packet dropped from the height $x_0 = 10$ above the mirror positioned at $x = 0$. The main difference appears to be enhanced spreading of the wave packet and strong interference with reflected waves in the linear model, as compared to the nonlinear case, where these phenomena are less pronounced.

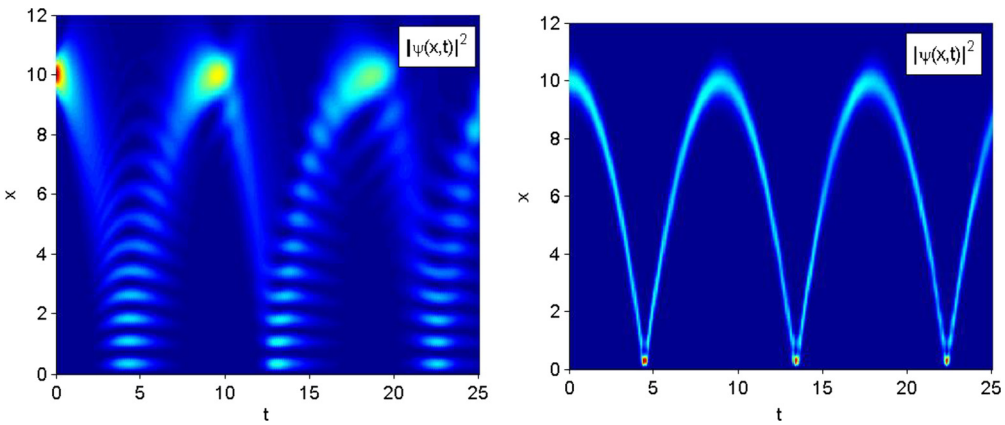

FIG. 1. (Color online) Left panel: The first three bouncings of the wave packet from the ideal mirror for the linear model ($\gamma = 0$) is shown through the density plot $|\psi(x,t)|^2$. Right panel: The same for the nonlinear model ($\gamma = 1$). In both cases a wave packet $\psi(x,0) = A\exp[-(x-x_0)^2/a^2]$ with $A = 2$, $a = 0.8$, and $x_0 = 10$ has been employed as the initial condition for the governing Eq. (3), with the coefficient of linear potential $\alpha = 1$.

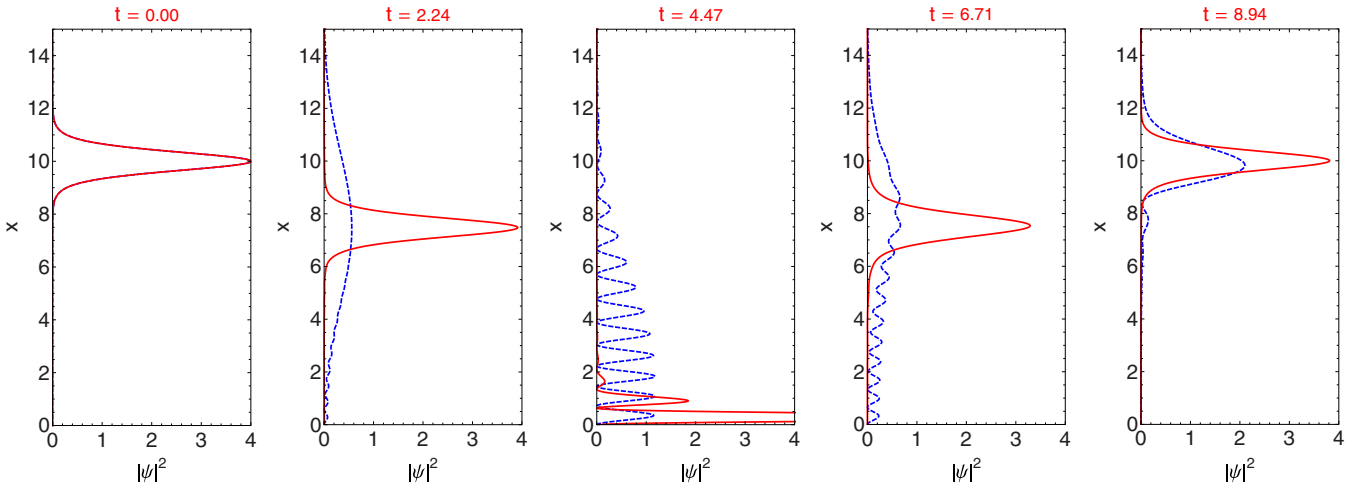

FIG. 2. (Color online) Snapshots of the wave packet dropped from the height $x_0 = 10$ at different times (shown on top of each figure) during one bouncing period $T_b = 8.94$. In the linear model the wave packet quickly expands and shows strong interference with waves reflected by the mirror placed at $x = 0$ (blue dashed line). At final time T_b the wave packet does not fully recover its initial form. In the nonlinear case the wave packet better keeps its integrity during the evolution and almost fully recovers its initial form at T_b (red solid line). All parameters are the same as in the previous figure.

The distinctions between the two models are clearly observed in Fig. 2, where we compare the corresponding wave profiles at different times during one period of bouncing T_b, which is estimated from the classical equation $d^2x/dt^2 = -g$. In dimensionless units introduced for Eq. (3) we need to set $g = 1$. Then a classical particle dropped from the height x_0 reaches the ground at $t_b = \sqrt{2x_0}$, therefore the classical bouncing period is $T_b = 2t_b = 2\sqrt{2x_0}$.

It should be noted that in Fig. 2 we show the situation, when the wave packet is dropped from a quite great height and the effect of gravity is maximal ($\alpha = 1$). This gives rise to notable deformation of the nonlinear wave packet also, in proximity of the mirror (see the middle panel). After the instant interaction with the mirror at $t = T_b/2$, the soliton quickly recovers its form. Asymmetric deformation of the wave packet and emergence of side peaks (interference fringes) during the evolution are the main factors compromising the precision of analytical description developed in the next section.

To estimate the parameters of the model we consider the ^{85}Rb condensate, for which $a_s = -20$ nm, $l_g \approx 1.3\,\mu$m, $t_g = 0.36$ ms. At the strength of radial confinement $\omega_\perp = 10^3$ rad/s we have $\gamma = 1$. For $N = 4$ the soliton contains ≈ 720 atoms. Similar estimates for ^{7}Li condensate with $a_s = -1.6$ nm give $l_g \approx 7\mu$m, $t_g = 0.84$ ms, $\omega_\perp = 10^4$ rad/s; the soliton contains ≈ 1400 atoms.

III. VARIATIONAL APPROXIMATION

For arbitrary forms of the reflecting potential $V(x)$, the governing Eq. (3) cannot be analytically investigated. One of the efficient approaches to the problem in such cases is the variational approximation (VA), first developed for pulse propagation in optical fibers [24], and later applied to many other areas of nonlinear physics [25].

Below we develop the VA for the governing equation using the second choice (b) for the potential Eq. (4). It is well known from quantum mechanics textbooks that the wave packet falling on the δ potential barrier is always partially transmitted. However, by increasing the strength of the barrier (V_0) the transmission coefficient can be reduced to a negligible level. This allows us to consider the norm of the wave packet above the mirror as a conserved quantity and develop the VA using an appropriate ansatz for the pulse shape.

Equation (3) can be generated from the following Lagrangian density:

$$\mathcal{L} = \frac{i}{2}(\psi\psi_t^* - \psi^*\psi_t) + \frac{1}{2}|\psi_x|^2 + \alpha\, x\,|\psi|^2 - V(x)|\psi|^2 - \frac{\gamma}{2}|\psi|^4. \tag{5}$$

An important step in the development of VA is the proper choice of the trail function. We shall consider the following hyperbolic secant ansatz

$$\psi(x,t) = A\ \mathrm{sech}\left(\frac{x-\zeta}{a}\right) e^{ib(x-\zeta)^2 + i\xi(x-\zeta) + i\varphi}, \tag{6}$$

where $A(t), a(t), \zeta(t), \xi(t), b(t), \varphi(t)$ are variational parameters representing the amplitude, width, center-of-mass position, velocity, chirp parameter, and phase of the wave packet, respectively. This choice is motivated by the fact that when the wave packet is sufficiently far from the reflecting potential $V(x)$ (and therefore its effect can be neglected), Eq. (3) has the exact accelerated soliton solution of the hyperbolic secant form [26].

Substituting the ansatz (6) into Eq. (5) and integrating over the space variable we get the averaged Lagrangian $L = \int_{-\infty}^{\infty} \mathcal{L} dx$

$$L = N\left[\frac{\pi^2}{12}a^2 b_t + \frac{\pi^2}{6}a^2 b^2 - \frac{1}{2}\zeta_t^2 - \alpha\,\zeta + \varphi_t + \frac{1}{6a^2} + \frac{V_0}{2a}\,\mathrm{sech}^2\left(\frac{\zeta}{a}\right) - \frac{\gamma N}{6a}\right], \tag{7}$$

where we have taken into account that the velocity is equal to the time derivative of the center-of-mass position $\xi = \zeta_t$ and $A^2 = N/(2a)$, with the norm of the wave packet N being the conserved quantity. Now the usual procedure of the VA, applied to Eq. (7), leads to the following set of equations for the width and center-of-mass position of the wave packet

$$a_{tt} = \frac{4}{\pi^2 a^3} + \frac{6V_0}{\pi^2 a^2}\,\mathrm{sech}^2\left(\frac{\zeta}{a}\right)\left[1 - \frac{2\zeta}{a}\tanh\left(\frac{\zeta}{a}\right)\right] - \frac{2\gamma N}{\pi^2 a^2}, \tag{8}$$

$$\zeta_{tt} = -\alpha + \frac{V_0}{a^2}\,\mathrm{sech}^2\left(\frac{\zeta}{a}\right)\tanh\left(\frac{\zeta}{a}\right). \tag{9}$$

The coupled system of equations (8) and (9) represents the main result of this paper. Its fixed points provide the stationary width of the soliton (a_0) and its distance from the mirror (ζ_0), where the actions of the gravity and repulsive potential $V(\zeta)$ cancel each other. As a result of this balance, the soliton placed at a fixed point remains at rest (levitates) above the mirror. Small amplitude dynamics of the soliton's width and center-of-mass position near the stationary state can be described as the motion of a unit mass particle in the anharmonic potentials $U_1(a)$ and $U_2(\zeta)$, respectively,

$$a_{tt} = -\frac{\partial U_1}{\partial a}, \quad U_1(a) = \frac{2}{\pi^2 a^2} - \frac{2\gamma N}{\pi^2 a} - \frac{6V_0}{\pi^2 a}\,\mathrm{sech}^2\left(\frac{\zeta_0}{a}\right), \tag{10}$$

$$\zeta_{tt} = -\frac{\partial U_2}{\partial \zeta}, \qquad U_2(\zeta) = \alpha\,\zeta + \frac{V_0}{2a_0}\,\mathrm{sech}^2\left(\frac{\zeta}{a_0}\right). \tag{11}$$

In Fig. 3 the shapes of the potentials in Eqs. (10) and (11) and the examples of soliton bouncing dynamics over the reflecting surface, modelled by a delta function, are illustrated. As expected, when the soliton is positioned at a fixed point (ζ_0, a_0), it stays motionless (lower pair of curves in the middle panel). Small amplitude oscillations in partial differential equation (PDE) data are due to the fact that the VA gives approximate values for the fixed point. When the soliton is dropped towards the mirror from a height $x_0 = 3$, it performs a bouncing motion. The slow decay of the amplitude of oscillations and increase of its bouncing frequency are due to the partial escape of the wave packet via tunnel effect (upper pair of curves in the middle panel).

The frequency of small amplitude oscillations of the soliton's motion can be estimated from VA by linearizing Eqs. (8) and (9) near the fixed point (ζ_0, a_0)

$$\omega_0 = \left(V_0/a_0^3\right)^{1/2}\mathrm{sech}^2(\zeta_0/a_0)[2\sinh^2(\zeta_0/a_0) - 1]^{1/2}. \tag{12}$$

The corresponding period for $V_0 = 1$, $\zeta_0 = 1.213$, and $a_0 = 0.468$ is $T_0 = 2\pi/\omega_0 \simeq 9.7$. This is in quite good agreement with numerical simulations of the GPE (3) for the equilibrium state, shown in the middle panel of Fig. 3. An expression similar to Eq. (12) can be derived for the frequency of the soliton's width

$$\Omega_0 = \left(2/\pi a_0^2\right)\{3 - \gamma N a_0 + (3V_0/a_0)\,\mathrm{sech}^2(\zeta_0/a_0) \times [a_0^2 + 2\zeta_0^2 - 4a_0\zeta_0\tanh(\zeta_0/a_0) - 3\zeta_0^2\mathrm{sech}^2(\zeta_0/a_0)]\}^{1/2}. \tag{13}$$

The numerical estimate for the fixed point (ζ_0, a_0), and $N = 4$, $\gamma = 1$, $V_0 = 1$ is $T_0 = 2\pi/\Omega_0 = 1.94$, which is also in good agreement with the results of GPE.

When a mathematical model has been developed, it is appropriate to mention its range of validity. As pointed out in the previous section, hard bounces of the soliton lead to its asymmetric deformation at the instant of collision with the mirror. Deviation of the waveform from the class of selected ansatz Eq. (6) is the main factor compromising the accuracy of the variational approach. Therefore, the validity of the analytical model developed in this section is limited to the domain of *soft collisions* (at small velocity) and *dense* (tall and narrow) wave packets. These conditions are satisfied when the effect of gravity is reduced ($\alpha \ll 1$) and the soliton contains a large number of atoms, so that the nonlinearity-induced self-focusing of the wave packet is significant.

The variational approach is especially useful when small amplitude oscillations of the wave packet near its equilibrium position are the subject of interest. In this case the analytic

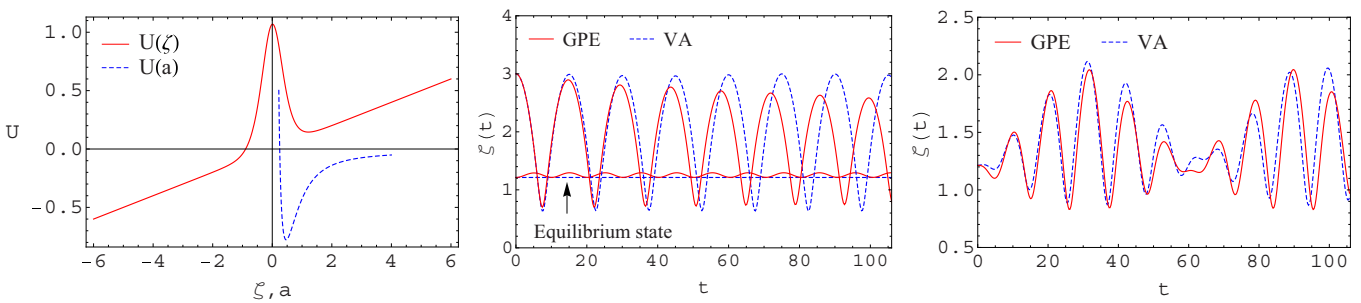

FIG. 3. (Color online) Left panel: Anharmonic potentials for the center of mass $U(\zeta)$ and width $U(a)$ of the soliton, according to Eqs. (10) and (11). For the set of parameters $N = 4$, $\gamma = 1$, $\alpha = 0.1$, and $V_0 = 1$ the fixed point is found to be $\zeta_0 = 1.213$, $a_0 = 0.468$. Middle panel: Comparison of the center-of-mass position as a function of time, obtained from solving the VA Eq. (8) and numerical simulation of the governing Eq. (3) for the reflecting surface of the δ function type $V(x) = \alpha\,x$. The lower pair of curves correspond to the fixed point initial conditions, while the upper pair of curves correspond to dropping the wave packet from height $x_0 = 3$ above the mirror. Right panel: Nonlinear resonance in the center-of-mass dynamics when the coefficient of gravity is varied in time with a resonance frequency $\alpha(t) = 0.1[1 + 0.3\sin(\omega_0 t)]$. Stationary state of the soliton with parameters predicted by VA is used as initial condition. Discrepancy (phase shift) between the GPE and VA is associated with asymmetric deformation of the wave packet when reflecting from the mirror.

formulas for the frequency of oscillations for the center-of-mass Eq. (12) and width Eq. (13) are quite accurate. If the relevant experiment shows deviation from the prediction of these formulas that will be an indication of the presence of additional forces acting on the soliton near the surface. Actually, the experiments with BEC aimed at exploring the Casimir-Polder force near the surface use the perturbations of the frequency of center-of-mass oscillations of the condensate to detect this force [9]. Similar experiments with attractive BEC in the bouncing soliton regime would be very informative.

IV. FERMI-TYPE ACCELERATION OF A MATTER-WAVE SOLITON

The capability of the matter-wave soliton to perform a bouncing motion above the atomic mirror, preserving its integrity, suggests considering the Fermi-type acceleration (FA) in this system. FA is the energy gained by a particle exposed to periodic or random driving forces. It was proposed by Fermi [27] to explain why cosmic rays have such high energy. For the mechanical analog, the possibility of unbounded growth of energy by an elastic ball bouncing vertically on a single periodically oscillating plate, under the effect of gravity, was rigorously proven by the authors of [28]. A simple derivation of the growth rate of the ball's velocity in the framework of classical mechanics ($v \sim t^{1/3}$) can be found in [29]. Most studies of FA of matter waves are concerned with dynamical localization and chaotic behavior. In our model the localization of the matter wave naturally arises from the nonlinearity of the condensate, and the parameter space does not contain chaotic regions.

Although the matter-wave soliton does not have all the necessary properties to demonstrate true FA (due to nonelastic collision with the mirror, leakage of energy via tunnel effect, etc.), nevertheless some features of FA can be observed, as we have revealed in the numerical experiments. At first we need to prepare the initial stationary state of the matter wave packet levitating above the atomic mirror. The prediction of VA for parameters of the soliton and stationary state distance above the mirror (where the forces of gravity and repulsion of the mirror balance out) is approximate, as we have seen in the previous section. The inaccuracy leads to small amplitude oscillations of the soliton near the equilibrium state in the GPE simulations (see middle panel in Fig. 3). To create a truly stationary initial state of the soliton above the reflecting surface we consider the first choice (a) for $V(x)$ in Eq. (4). For this ideal mirror potential, the Eq. (3) in the linear limit ($\gamma = 0$), with boundary condition $\psi(0,t) = 0$, has analytic stationary solutions in terms of the Airy functions [30]

$$\psi_n(x) = \mathcal{N}\,\mathrm{Ai}[(2\alpha)^{1/3}\,(x + x_n)], \tag{14}$$

where $\mathcal{N}$ is some normalization constant. Below we shall be concerned with the ground state ($n = 0$) of the wave packet in the gravitational cavity. The first root, given by $\mathrm{Ai}[(2\alpha)^{1/3}x] = 0$ for $\alpha = 0.1$, is found to be equal to $x_0 = -3.998$. The corresponding normalization factor is

$$\mathcal{N} = \left(\int_0^\infty \mathrm{Ai}^2[\alpha^{1/3}(x + x_0)]dx\right)^{-1/2} = 1.09. \tag{15}$$

To produce the initial state for numerical simulations of the Fermi acceleration we insert the ground-state wave function (14) with appropriate norm into the GPE (3) with $\gamma = 0$ and slowly raise it to the final value $\gamma = 1$ according to the law $\gamma(t) = \tanh(5t/t_0)$ with $t_0 \sim 1000$. The obtained nonlinear waveform is shown in the left panel of Fig. 4. Also in this figure we illustrate the resonant oscillations of the soliton's center of mass when the coefficient of nonlinearity (via atomic scattering length) is periodically changed in time. It is evident that nonlinear resonance takes place at the frequency of small amplitude oscillations ω_0 estimated from the VA Eq. (12). Similar behavior was observed when the slope of the linear potential (strength of gravity) was changed with an appropriate frequency (see the right panel of Fig. 3). Since the resonant frequencies are different for the center of mass (ω_0) and width (Ω_0) of the soliton, periodic modulation of the parameter α or γ with frequency ω_0 do not induce resonant oscillations of the width and vice versa. A characteristic feature inherent to both cases is that oscillations show notable phase shift as compared to predictions of VA, which can be explained by asymmetric deformation of the soliton at the impact with the reflecting surface. In the VA we deal with the dynamics of a unit mass particle in the anharmonic potential. Nevertheless the VA provides a qualitatively correct description of the system.

The focusing nonlinearity, inherent to BEC with negative s-wave scattering length, provides the wave packet's

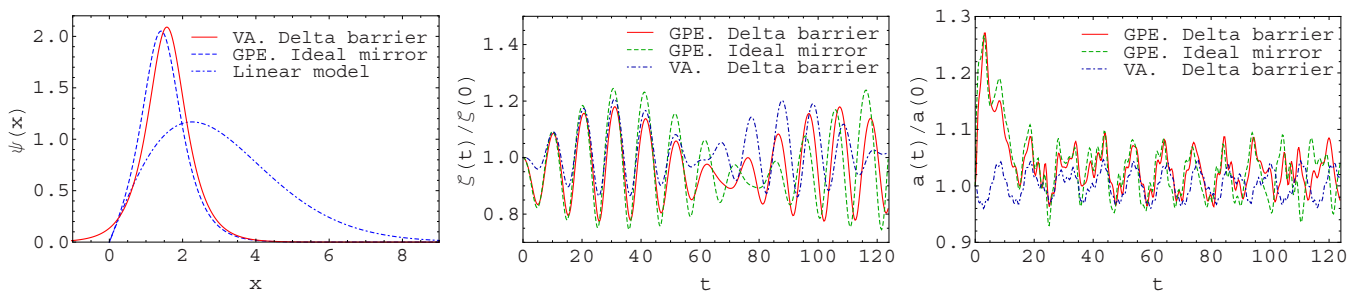

FIG. 4. (Color online) Left panel: Transformation of the ground-state wave function of the linear problem (blue dot-dashed line) into solution of the nonlinear problem (blue dashed line) by slowly raising the coefficient of nonlinearity γ in Eq. (3) from zero to one. In the prediction of the VA Eqs. (8) and (9) for δ barrier potential (red solid line) the wave packet slightly penetrates into the region $x < 0$ due to the wave tunneling effect. Middle panel: Nonlinear resonance in the center-of-mass dynamics of the soliton, when the coefficient of nonlinearity is periodically varied in time $\gamma = 1 + \epsilon\sin(\omega_0 t)$. Right panel: Dynamics of the width has not resonant character due to the difference in frequencies Ω_0 and ω_0, estimated from Eqs. (12) and (13). Parameter values $N = 4$, $\alpha = 0.1$, $V_0 = 5$, $\epsilon = 0.05$, $\omega_0 = 0.66$, $\Omega_0 = 1.7$.

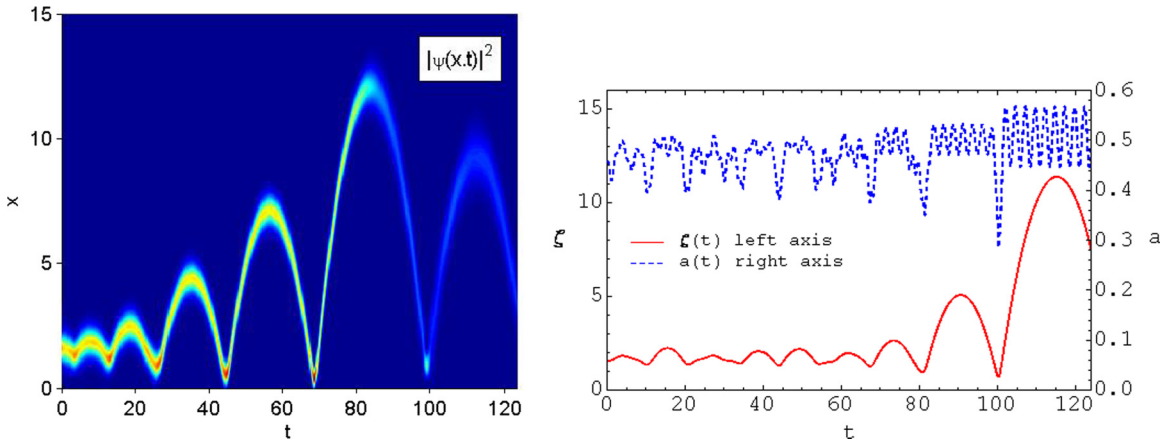

FIG. 5. (Color online) Left panel: Soliton continuously increases its kinetic energy and further departs from the stationary point $x_0 = 1.57$, when the vertical position of the δ function mirror with strength $V_0 = 5$, initially positioned at $x = 0$, is periodically changed at a parametric resonance frequency $f(t) = \varepsilon \sin(\Omega t)$, with $\varepsilon = 0.25$, $\Omega = 2\,\omega_0$, $\omega_0 = 0.66$, according to numerical simulations of the GPE (3). As the amplitude of the oscillations increases, the detuning from the resonance occurs and energy gain reverses. Right panel: Corresponding prediction of the VA for the soliton's center of mass and width. A qualitative agreement with the results of the GPE is observed.

robustness against dispersive spreading and different kinds of perturbations. Due to this property, matter-wave solitons keep their integrity after reflection from the atomic mirror. Below we consider the possibility of a Fermi-type of acceleration in the system. In numerical simulations we take the stationary state of the wave packet, predicted by VA as the initial condition for Eq. (3) and periodically change the vertical position of the reflecting surface or the slope of the linear potential.

Figure 5 illustrates the progressive gain of energy by the soliton when the position of the reflecting δ potential is periodically varied in time at a parametric resonance frequency. As the amplitude of the oscillation above the mirror increases, detuning from the resonance occurs and a further gain of energy stops. A proper synchronization would allow more increase of the kinetic energy of the soliton. Also there is a contribution of tunnel loss of the wave packet through the reflecting δ potential barrier.

The corresponding predictions of the VA for the center-of-mass position ζ and width a are also shown on the right panel of Fig. 5. Note that the space coordinate in GPE and VA equations are designated by x and ζ, respectively. Variation of the vertical position of the δ function mirror $V(x) = V_0\,\delta(x + f(t))$, where $f(t) = \varepsilon \sin(\Omega t)$ is a periodic function with amplitude ε and frequency Ω, leads to the VA equations, similar to Eqs. (8) and (9), but with a replaced space variable on the right-hand side $\zeta \to \zeta + f(t)$. The frequency of small amplitude oscillations of the width, measured at the upper turning point, is $T_0 \simeq 2.1$, which is close to the estimation from Eq. (13).

V. CONCLUSION

The model of a "quantum bouncer" has been extended to a nonlinear domain of Bose-Einstein condensates. The analytical description is based on the variational approach. It has been revealed that a matter-wave soliton bouncing above the reflecting surface (or atomic mirror) better preserves its integrity compared to a linear wave packet due to the focusing effect of the nonlinearity. This feature of the bright matter-wave soliton allows to develop a variational approach, using appropriate trial function, which provides a qualitatively correct description of its dynamics. A particle-like behavior of the matter-wave soliton bouncing above the atomic mirror is suggested to consider the Fermi-type acceleration in the system. In numerical experiments we observed the progressive energy gain by the soliton when the vertical position of the mirror is periodically varied in time. Further development of the proposed model may include the stochastic variation of the nonlinearity, the slope of the linear potential, and vertical position of the reflecting surface.

ACKNOWLEDGMENTS

This work has been supported by Project No. CG038-2013 of the University of Malaya. B.B.B. is grateful to the Department of Physics, University of Malaya, for the hospitality during his visit. F.A. acknowledges the support from Grant No. EDW B14-096-0981 provided by IIUM.

[1] J. J. Sakurai, *Modern Quantum Mechanics: Revised Edition* (Addison-Wesley, Reading, MA, 1994).
[2] S. Flügge, *Practical Quantum Mechanics I* (Springer, Berlin, 1971).
[3] R. L. Gibbs, Am. J. Phys. **43**, 25 (1975).
[4] J. Gea-Banacloche, Am. J. Phys. **67**, 776 (1999).
[5] P. W. Langhoff, Am. J. Phys. **39**, 954 (1971); R. D. Desko and D. J. Bord, *ibid.* **51**, 82 (1983); D. A. Goodings and T. Szeredi, *ibid.* **59**, 924 (1991); J. Gea-Banacloche, Opt. Commun. **179**, 117 (2000); S. Whineray, Am. J. Phys. **60**, 948 (1992); M. A. Doncheski and R. W. Robinett, *ibid.* **69**, 1084 (2001); R. W. Robinett, Eur. J. Phys. **31**, 1 (2010).

[6] M. Belloni and R. W. Robinett, Phys. Rep. **540**, 25 (2014).
[7] K. Bongs, S. Burger, G. Birkl, K. Sengstock, W. Ertmer, K. Rzążewski, A. Sanpera, and M. Lewenstein, Phys. Rev. Lett. **83**, 3577 (1999); H. Perrin, Y. Colombe, B. Mercier, V. Lorent, and C. Henkel, J. Phys. B: At. Mol. Opt. Phys. **39**, 4649 (2006); V. Savalli, D. Stevens, J. Esteve, P. D. Featonby, V. Josse, N. Westbrook, C. I. Westbrook, and A. Aspect, Phys. Rev. Lett. **88**, 250404 (2002).
[8] T. A. Pasquini, Y. Shin, C. Sanner, M. Saba, A. Schirotzek, D. E. Pritchard, and W. Ketterle, Phys. Rev. Lett. **93**, 223201 (2004); T. A. Pasquini, M. Saba, G. Jo, Y. Shin, W. Ketterle, D. E. Pritchard, T. A. Savas, and N. Mulders, *ibid.* **97**, 093201 (2006); C. Lee and J. Brand, Europhys. Lett. **73**, 321 (2006); S. L. Cornish *et al.*, Physica D **238**, 1299 (2009).
[9] D. M. Harber, J. M. Obrecht, J. M. McGuirk, and E. A. Cornell, Phys. Rev. A **72**, 033610 (2005); J. M. Obrecht, R. J. Wild, M. Antezza, L. P. Pitaevskii, S. Stringari, and E. A. Cornell, Phys. Rev. Lett. **98**, 063201 (2007); F. Sorrentino, A. Alberti, G. Ferrari, V. V. Ivanov, N. Poli, M. Schioppo, and G. M. Tino, Phys. Rev. A **79**, 013409 (2009).
[10] V. V. Nesvizhevsky *et al.*, Nature (London) **415**, 297 (2002); V. V. Nesvizhevsky, Phys. Usp. **47**, 515 (2004); Uspekhi Fizicheskikh Nauk **174**, 569 (2004); Phys. Usp. **53**, 645 (2010); Uspekhi Fizicheskikh Nauk **180**, 673 (2010).
[11] H. Abele and H. Leeb, New J. Phys. **14**, 055010 (2012).
[12] G. Ichikawa, S. Komamiya, and Y. Kamiya, JPS Conf. Proc. **1**, 013101 (2014).
[13] A. Canaguier-Durand, A. Gérardin, R. Guérout, P. A. Maia Neto, V. V. Nesvizhevsky, A. Yu. Voronin, A. Lambrecht, and S. Reynaud, Phys. Rev. A **83**, 032508 (2011).
[14] G. Della Valle, M. Savoini, M. Ornigotti, P. Laporta, V. Foglietti, M. Finazzi, L. Duo, and S. Longhi, Phys. Rev. Lett. **102**, 180402 (2009).
[15] M. A. Doncheski and R. W. Robinett, Eur. J. Phys. **20**, 29 (1999); M. Belloni, M. A. Doncheski, and R. W. Robinett, Phys. Scr. **71**, 136 (2005).
[16] M. A. Kasevich *et al.*, Opt. Lett. **15**, 607 (1990); C. G. Aminoff, A. M. Steane, P. Bouyer, P. Desbiolles, J. Dalibard, and C. Cohen-Tannoudji, Phys. Rev. Lett. **71**, 3083 (1993); T. M. Roach, H. Abele, M. G. Boshier, H. L. Grossman, K. P. Zetie, and E. A. Hinds, *ibid.* **75**, 629 (1995); P. Szriftgiser, D. Guery-Odelin, M. Arndt, and J. Dalibard, *ibid.* **77**, 4 (1996); A. Landragin, J. Y. Courtois, G. Labeyrie, N. Vansteenkiste, C. I. Westbrook, and A. Aspect, *ibid.* **77**, 1464 (1996); A. Sidorov *et al.*, Quantum Semiclass. Opt. **8**, 713 (1996).
[17] T. Kohler, K. Goral, and P. S. Julienne, Rev. Mod. Phys. **78**, 1311 (2006); C. Chin, R. Grimm, P. Julienne, and E. Tiesinga, *ibid.* **82**, 1225 (2010).
[18] R. Ciurylo, E. Tiesinga, and P. S. Julienne, Phys. Rev. A **71**, 030701 (2005); M. Yan, B. J. DeSalvo, B. Ramachandhran, H. Pu, and T. C. Killian, Phys. Rev. Lett. **110**, 123201 (2013).
[19] F. Saif and I. Rehman, Phys. Rev. A **75**, 043610 (2007); F. Saif, K. Naseer, and M. Ayub, Eur. Phys. J. D **68**, 95 (2014).
[20] E. Granot and B. A. Malomed, J. Phys. B: At. Mol. Opt. Phys. **44**, 175005 (2011).
[21] G. A. Siviloglou, J. Broky, A. Dogariu, and D. N. Christodoulides, Phys. Rev. Lett. **99**, 213901 (2007); J. Broky, G. A. Siviloglou, A. Dogariu, and D. N. Christodoulides, Opt. Express **16**, 12880 (2008); I. D. Chremmos and N. K. Efremidis, J. Opt. Soc. Am. A **29**, 861 (2012); P. Chamorro-Posada, J. Sanchez-Curto, A. B. Aceves, and G. S. McDonald, Opt. Lett. **39**, 1378 (2014).
[22] M.-O. Mewes, M. R. Andrews, D. M. Kurn, D. S. Durfee, C. G. Townsend, and W. Ketterle, Phys. Rev. Lett. **78**, 582 (1997); V. Bolpasi, N. K. Efremidis, M. J. Morrissey, P. C. Condylis, D. Sahagun, M. Baker, and W. von Klitzing, New J. Phys. **16**, 033036 (2014).
[23] T. van Zoest *et al.*, Science **328**, 1540 (2010).
[24] D. Anderson and M. Lisak, Phys. Rev. A **27**, 1393 (1983).
[25] B. A. Malomed, in *Progress in Optics*, Vol. 43, edited by E. Wolf (Elsevier, Amsterdam, 2002), p. 69.
[26] H.-H. Chen and C.-S. Liu, Phys. Rev. Lett. **37**, 693 (1976).
[27] E. Fermi, Phys. Rev. **75**, 1169 (1949).
[28] L. D. Pustyl'nikov, Russ. Math. Surv. **50**, 145 (1995).
[29] G. M. Zaslavsky, *Stochasticity of Dynamical Systems* (Nauka, Moscow, 1984) [in Russian].
[30] O. Vallee and M. Soares, *Airy Functions and Applications to Physics* (Imperial College Press, London, 2004).